Controlled anisotropic deformation of Ag nanoparticles by Si ion irradiation

A. Oliver, J. A. Reyes-Esqueda, J. C. Cheang-Wong, C. E. Román-Velázquez, A. Crespo-Sosa, L. Rodríguez-Fernández, J. A. Seman, and Cecilia Noguez*

Instituto de Física, Universidad Nacional Autónoma de México, Apartado Postal 20-364, D.F. 01000, Mexico and REGINA: Red de Grupos de Investigación en Nanociencia, UNAM, Mexico

(Received 14 October 2005; revised manuscript received 2 October 2006; published 21 December 2006)

The shape and alignment of silver nanoparticles embedded in a glass matrix is controlled using silicon ion irradiation. Symmetric silver nanoparticles are transformed into anisotropic particles whose larger axis is along the ion beam. Upon irradiation, the surface plasmon resonance of symmetric particles splits into two resonances whose separation depends on the fluence of the ion irradiation. Simulations of the optical absorbance unambiguously show that the anisotropy is caused by the deformation and alignment of the nanoparticles, and that both properties are controlled with the irradiation fluence.

DOI: 10.1103/PhysRevB.74.245425 PACS number(s): 61.72.Ww, 73.20.Mf, 78.67.Bf

I. INTRODUCTION

Nanosized metal particles exhibit optical surface plasmons that have revealed new aspects for applications in photonics devices.[1,2] Surface plasmons are tailored by altering the surface of nanoparticles (NPs) in some way.[3,4] The potential applications of NPs depend on the ability to control their size, shape, and environment. Thus new synthesis methods have been developed, like the ion implantation technique, which is very versatile due to the possibility of fabricating both metal and semiconductor NPs embedded in a variety of host matrices.[5,6] This method has advantages over other techniques, because of the high control on the distribution and concentration of impurities, allowing the growth of NPs in a well-defined space region of the host matrix, such that buried channel waveguides are directly formed.[5] Besides, high concentrations of metal NPs can be reached, yielding values for the third-order nonlinear optical susceptibility much larger than those found in other metal-doped solids.[7] On the other hand, to obtain a second-order nonlinear optical response, a macroscopic noncentrosymmetry must be induced in some way, since nanocomposites are isotropic and centrosymmetric. Up to now, only very small second harmonic generation signals have been measured.[8]

Anisotropic deformation of silica using MeV ion irradiation has been observed.[9] Also, ion irradiation in the keV–MeV energy range for micrometer-sized colloidal silica particles was employed to change their shape from spheres into oblate spheroids.[10,11] In the same way, gold NPs of 14 nm diameter surrounded by a silica shell of 72 nm diameter irradiated with 30-MeV Se ions have been deformed.[12] In this case, the spherical shell was deformed into an oblate spheroid, such that its major axis was in the direction perpendicular to the ion beam, while the Au core was deformed into a nanorod in the parallel direction. However, deformation of transition-metal NPs had not been observed previously to the original submission of the present paper, although some attempts had been made. Furthermore, despite the large effort made to date,[9–14] rigorous procedures to control the deformation of embedded metal NPs using ion-beam irradiation have not been established. For instance, Ag particles of few nanometers embedded in a planar sodalime glass film were irradiated with 30-MeV Si ions, producing chains of NPs aligned along the ion-beam direction, but no shape deformation was observed.[13,14] During the revision of the present paper, recent work in this direction has been published.[15] Penninkhof and collaborators reported that Au implanted in planar SiO_2 films at low temperature (77 K) with typical colloid diameters of 5–20 nm, after irradiation with 30-MeV Si ($9.3\times10^{14}/cm^2$) showed a clear deformation of the Au colloids as observed by transmission electron microscopy (TEM).[15] They also reported results for Ag implanted in planar SiO_2 films with a large density of much smaller colloids. Contrary to gold, they reported no deformation of the Ag colloids after irradiation under the same conditions.[15]

In this work, we demonstrate that the shape and alignment of Ag NPs with diameters of about 5 nm embedded in a glass matrix are controlled using silicon ion irradiation. Symmetric silver nanoparticles are transformed into anisotropic particles whose larger axis is along the ion beam. In our case, the samples were irradiated at room temperature with Si ions at a smaller energy (8 MeV) but using larger fluences ($0.1–2.0\times10^{16}$ Si/cm^2). Our samples were characterized by using optical techniques, which are nondestructive and with a proper implementation, they can be used to perform measurements *in situ* and in real time, providing statistical properties of the whole sample. These attributes of optical spectroscopies are crucial because the properties of nanoparticles depend on the environment, and when growth and characterization are made in different ambient conditions, this might be an additional uncontrollable variable during fabrication and for their interpretation. Furthermore, optical spectroscopies have advantages over other tools for characterization as structural characterization techniques like TEM, which only provides the image of a small piece of the sample, giving information only about local properties and characterizing few NPs at a time.

In this work, we also show that the ion irradiation not only induces anisotropic deformation of silver NPs, but also that this deformation can be controlled with the fluence of the ion beam. Theoretical simulations of the optical-absorption data show that the polarization dependence of the surface plasmons is in agreement with models for prolate silver NPs. High-resolution transmission electron micros-

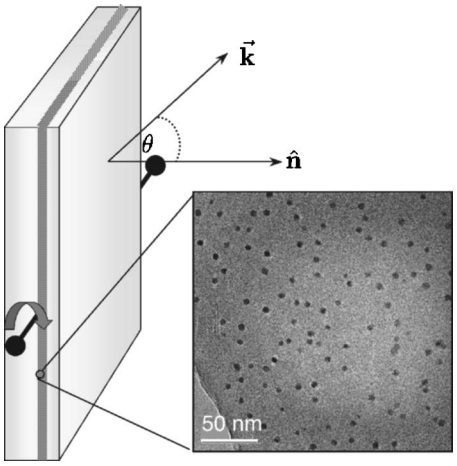

FIG. 1. Schematic model of the nanocomposite and a HRTEM micrograph.

copy (HRTEM) also shows that the NPs do not form chains in any direction after irradiation. Therefore we conclude that the anisotropic optical response of the nanocomposite is attributed only to the deformation and alignment of the silver NPs, which are controlled with the ion-beam fluence.

II. SYNTHESIS AND DEFORMATION OF SILVER NANOPARTICLES

Using high-purity silica glass plates ($20\times20\times1$ mm^3), NSG ED-C (Nippon silica glass) as host matrices, Ag nanoparticles are synthesized by implanting 2-MeV Ag^{2+} ions at room temperature. The silica plates have no individual impurity content greater than 1 ppm, with less of 1 ppm of OH and a total impurity content less than 20 ppm. The system is then thermally annealed at 600 °C in a 50% N_2+50% H_2 reducing atmosphere. The Ag-ion fluence and projected range are of 5×10^{16} Ag/cm^2 and 0.9 μm, respectively, as measured by Rutherford backscattering spectrometry (RBS). Ion implantation and RBS analysis were performed at the 3-MV Tandem accelerator (NEC 9SDH-2 Pelletron). An Ocean Optics Dual Channel S2000 UV-visible spectrophotometer was used to collect the optical-absorption spectra, which shows the formation of silver NPs,[6] with a single narrow surface plasmon located at 391 nm with a full width at half maximum (FWHM) of about 41 nm, which is characteristic of spherical-like shaped NPs of 6 nm diameter.[4]

Afterwards, the silica plate was cut into pieces and each piece was irradiated at room temperature with 8-MeV Si ions. According to our previous results concerning the ion-beam-induced deformation of silica particles,[16] 8-MeV Si ions were chosen, since their electronic stopping power for SiO_2 is 200 times higher than the nuclear one. On the other hand, the ion projected range for this energy is 4.3 μm in SiO_2, i.e., far beyond the location of the Ag NPs. The Si irradiation was performed under an angle off normal of $\theta=-41°$. Each sample was irradiated at different Si fluences in the range of $0.1-2.0\times10^{16}$ Si/cm^2 in order to induce a deformation in the Ag NPs.

On the left-hand side of Fig. 1, a schematic model of the buried region into the glass sample containing the silver NPs is shown. The incident ion beam makes an angle $\theta=-41°$ with the normal $\hat{\mathbf{n}}$. We performed HRTEM studies using a JEOL 2010F at 200 kV, by uncapping the sample for both sides in the direction of the surface normal until few hundreds of nanometers, employing an ion-beam milling. On the right-hand side of Fig. 1 a HRTEM micrograph of the in-normal view of the irradiated sample shows that the silver NPs are randomly located, i.e., they do not form chains or any other kind of arrangement. The size distribution of the implanted sample was obtained from a digitalized amplified micrograph by measuring the diameter of each NP. The size distribution obtained from the statistic over 290 NPs shows a diameter distribution centered at 5.9 nm with a standard deviation of 1.1 nm. One should notice from the micrograph the homogeneity of size and distribution of the NPs in the sample.

III. RESULTS

The optical absorbance of the nanocomposites has been measured by varying the angle θ of the wave vector $\vec{\mathbf{k}}$ of the incident electromagnetic field with respect to $\vec{\mathbf{n}}$, as shown in Fig. 1. The polarization of the incident electric field was varied at different angles ϕ with respect to the horizontal axis passing on the sample plane and perpendicular to $\vec{\mathbf{k}}$. In Fig. 2 we present the absorbance for a nanocomposite after Si irradiation with a fluence of 0.5×10^{16} Si/cm^2. In Fig. 2(a) the absorption spectra for $\theta=0°$ are shown. When $\phi=0°$, a surface plasmon resonance at about 375 nm is observed. As the angle of polarization increases, the intensity of this first resonance decreases and a new peak appears at about 470 nm and becomes more intense, dominating the spectra at $\phi=90°$. Notice that the first resonance is small but not null when $\phi=90°$.

Figures 2(b) and 2(c) show the absorbance of the same composite, but with $\vec{\mathbf{k}}$ at $\theta=+45°$ and $-45°$, respectively. When $\theta=+45°$, the spectra show the same behavior as described above for $\theta=0°$, except that when the polarization angle is $\phi=90°$, the first resonance at 375 nm completely disappears. Conversely, when the incidence angle is $\theta=-45°$ the resonance at 375 nm is present for any ϕ, and its intensity shows small variations. In this case, the resonance at 470 nm is always less intense, and for $\phi=0°$ is null. From the spectra, we observe that the resonance at 470 nm disappears always for one polarization ($\phi=0°$), for any angle θ of the incident electromagnetic field. All these results mean that the optical response of the system is anisotropic and has only one axis of symmetry. Furthermore, this axis should be along the direction related to the resonance at 470 nm. It is concluded that this optical behavior is qualitatively reproduced and explained by simply considering the NPs as prolate spheroids.

IV. DISCUSSION

A. Optical properties

To corroborate the last statement of the results, the optical-absorbance spectra were simulated by employing

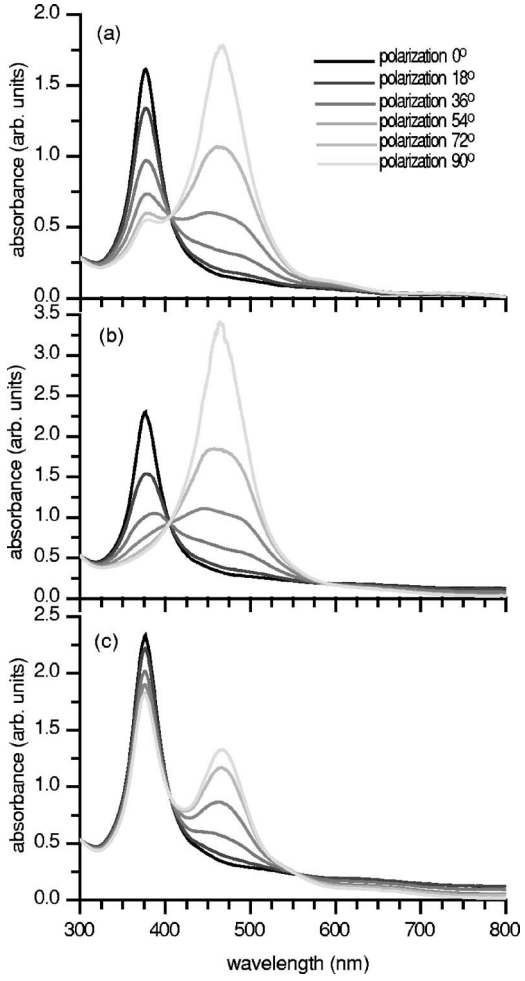

FIG. 2. Measured optical absorbance for linear-polarized light from 0° to 90°, and (a) θ=0°, (b) θ=+45°, and (c) θ=−45°. The polarization is indicated in the first plot, and is the same for all plots.

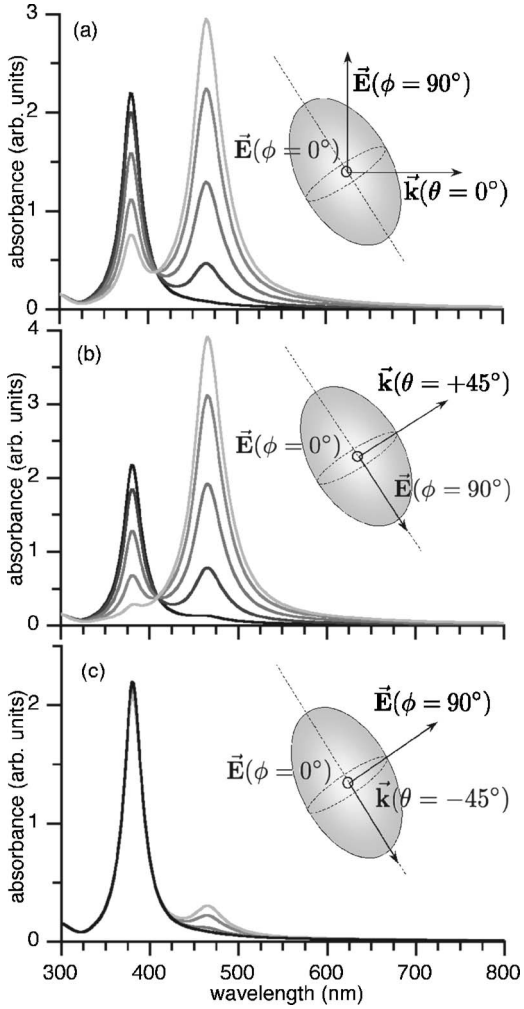

FIG. 3. Simulated absorbance spectra of prolate spheroids for linear-polarized light from 0° to 90°, and (a) θ=0°, (b) θ=+45°, and (c) θ=−45°. The polarization is the same as indicated in Fig. 2. The orientation of the major axis with respect to the incident electromagnetic field is depicted.

prolate spheroids whose symmetry axis is along the major axis, as depicted in Figs. 3(a)–3(c). Since we are mainly interested in silver NPs, whose sizes are smaller than 10 nm, radiation effects, such as scattering and radiation damping, are negligible, and the particle absorbs energy through the excitation of surface plasmon resonances mainly.[4] Then, the optical absorbance was simulated by calculating the induced polarization on the particle within the quasistatic approximation for spheroids with different aspect ratio a/b, among its major a, and minor b axes.[3] We employed the measured dielectric function for bulk silver,[17] where the main effects at the appropriate scale were incorporated. For instance, we have to consider that the conduction electrons suffer an additional damping effect due to surface dispersion or finite size. In such case, we have to make an additional adaptation to the measured dielectric function for bulk silver, including an extra damping term, which depends on the size of the NP.[4] The macroscopic dielectric function has contributions from interband and intraband electron transitions, such that, below 320 nm, the light absorption is mainly due to the interband electronic transitions of silver. This feature is quite independent of the shape and size of the NPs, as it was actually corroborated in all the experimental spectra. In contrast, a Drude like model of free electrons describes the intraband electron transitions, which are responsible of the surface plasmon resonances.[4] Besides, the NPs concentration on the matrix is small, so the interactions between NPs are negligible. As a result of all these considerations, it is valid to model the absorbance of the nanocomposite as the optical response of one embedded Ag NP weighted with the particle's concentration.

It was found that prolate spheroids with an aspect ratio of a/b=1.615 and a major axis of 8 nm reproduce very well the main features of the experimental optical spectra. This aspect ratio explains why it is difficult to observe the deformation in the micrographs at first glance, since they are taken at an angle of about −41° from the major axis of the NPs. In this case, the projected deformation of about 1.16 coincides with the small differences between the larger and smaller axes observed with HRTEM. In any case, it is difficult to conclude that NPs are deformed from the micrographs only, and we should remind that techniques like TEM only provides the

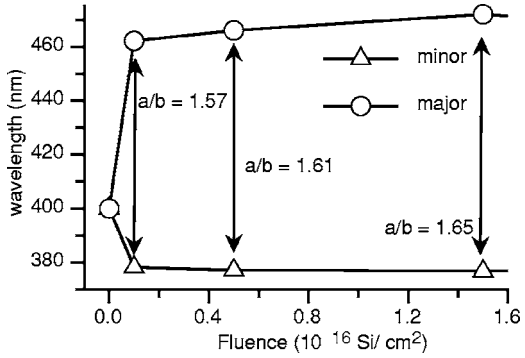

FIG. 4. Plasmon resonance position as a function of the Si-ion fluence. The measurement was made with $\theta=+45°$, and light polarized at $\phi=0°$ and 90°.

image of a small piece of the sample, giving partial information, while optical absorption provides us the properties of the whole sample.

Figures 3(a)–3(c) shows the simulated absorbance spectra for the incident electromagnetic field at $\theta=0°$, +45°, and −45°, and the same angles of polarization as in the experiment. When $\theta=0°$ in Fig. 3(a), it is observed that $\vec{\mathbf{k}}$ makes an angle of about 50° with the major axis, and for $\phi=0°$ the electric field is along the minor axis exciting only the surface plasmon at 375 nm. Conversely, when the angle of polarization is $\phi=90°$, both resonances are excited, but the one at 375 nm is weaker than the resonance at 470 nm. Similarly, when $\theta=+45°$ in Fig. 3(b), the wave vector $\vec{\mathbf{k}}$ is almost aligned to one of the minor axes, in consequence, the electric field is polarized along the other minor axis at $\phi=0°$, and along the major axis at $\phi=90°$. Finally, when $\theta=-45°$ in Fig. 3(c), the wave vector $\vec{\mathbf{k}}$ is along the major axis, in such a way that the electric field mostly excites the resonance at 375 nm for any polarization. Since $\vec{\mathbf{k}}$ and the major axis are not completely aligned, because the implantation was done at an angle −41° off-normal, small contributions from the second resonance at 470 nm are observed. The simulated spectra are in very good agreement with the experimental measurements. Therefore it is concluded that silver NPs suffer a deformation due to MeV Si ion irradiation that can be explained in terms of aligned prolate spheroids.

When the fluence of the Si-ion irradiation varies systematically from 0.1 to 2.0×10^{16} Si/cm^2, the behavior of the absorbance for all nanocomposites, as a function of the angles of incidence θ and polarization ϕ, is the same as the one described above. However, as it is shown in Fig. 4, as the Si-ion irradiation fluence increases, the resonance below 400 nm shifts to lower wavelengths, while the resonance above 400 nm shifts to larger ones. This separation between resonances is also explained in terms of aligned prolate spheroids: as the aspect ratio between major and minor axes increases, the separation among resonances also does. The resonance along the larger axis of prolate particles, called the longitudinal mode, is displaced to larger wavelengths as the aspect ratio increases, while the transversal resonance is shifted to smaller wavelengths. It is known that for small aspect ratios the longitudinal resonance shows a linear behavior, where the slope depends on the refraction index of the matrix. On the other hand, the transversal resonance is inversely proportional to the aspect ratio, showing a limit wavelength value that depends on the plasma frequency of the metal and the refraction index of the matrix.[18] Therefore as the irradiation fluence increases, it is concluded that the NPs' anisotropic deformation increases as well.

B. Deformation mechanism

From the optical spectra, it is clear that silver NPs are deformed into prolates spheroids with their major axis along the ion-beam direction. Notice that this effect has not been observed previously for silver NPs,[15] and only the formation of chains could be observed.[13,14] On the other hand, the deformation mechanism has been noticed for cobalt NPs implanted in SiO_2 and irradiated with iodine,[19] and recently, in gold NPs implanted in planar SiO_2 films after irradiation with Si[15] and Cu ions.[20] However, it is remarkable that silver NPs under the same conditions as gold were not deformed after irradiation.[15]

The deformation mechanism in all these cases is still unspecified, although some insights have been outlined.[19,21] For many years, the plastic flow model had been successfully used to understand the anisotropic deformation of amorphous materials subjected to irradiation with ions at energies of ~0.1 MeV or higher.[22,23] One important condition established in this model is the existence of a stable noncrystalline phase of the material and one important result is that the expansion is perpendicular to the ion beam. As shown by previous works[15,20] and here, the plastic flow model cannot be applied directly to the metallic NPs, although some attempts have been done to use it qualitatively, indirectly in some cases, by considering that the metallic particle is elongated as a consequence of the compressive stress exerted by the viscoelastic deformation of the surrounding matrix.[12] Recently, an important refinement to this model was proposed by D'Orleans *et al.*[19] that invokes the mechanism of track formation combined with the plastic flow model, assuming that the NPs melt and flow into the ion track. One relevant result of this approach is the distinction of three different regions, when the temperature reached by the nanoparticle is plotted as a function of its radius. This temperature depends on the energy deposited by the ion as well as on the size of the particle. Here, we briefly explain the different regions proposed by D'Orleans *et al.*[19] to explain the deformation mechanism. A more complete review of the theoretical advances in this field as well as some of its limitations has been recently done by Klaumünzer.[21]

According to D'Orleans and collaborators,[19] in the first region for small particles, the ion deposits enough energy to raise the nanoparticle's temperature above the evaporation temperature, so that they explode and the fragments might re-grow into smaller NPs or be incorporated into other larger NPs. The later would happen by Ostwald ripening, provided that neighboring NPs are close enough to act as nucleating centers. In this region, NPs would grow in size symmetrically.[19] When the radius of the NP increases (region II), the energy deposited at the NP is enough to melt it only. The host matrix also responds to the thermal stress and there

is a plastic flow. But due to the differences in volume expansion and compressibility between the liquid metal and matrix, the particle suffers a creep deformation.[19] In region III, the NPs are large enough that they remain in their solid phase and no important shape deformation is found. This model, however, is limited by the fact that the processes described above occur in a first stage, within a time interval t, shorter than about 10^{-10} s.

To understand our results in terms of the D'Orleans and collaborators model, we calculate the temperature reached by silver NPs with 3 nm of radius irradiated with 8-MeV Si ions. We found that the temperature is in the intersection of regions I and II. On the other hand, our optical results suggest that the NPs volume remains almost constant during deformation, indicating that the deformation process could be occurring in region II, which means that NPs probably melt and flow into the ion track. However, we would not like to oversimplify this interpretation. For this purpose, we recall that the thermodynamics of the evaporated system may play an important role,[21] as well as the solubility and high mobility in the matrix of molten silver.[24] Thus we believe that a general picture of a compact, molten drop being deformed by the matrix is not precise, such that the consideration of a second stage involving times larger than 10^{-9} s is needed to take into account diffusion and relaxation processes occurring at lower, but still high, temperatures (400–900 K). One possible picture at this stage could include solid NPs surrounded by solute atoms, which could migrate to defect-rich regions, like those found along the ion tracks. In such a case, other experimental factors like irradiation temperature, NPs concentration, and atomic diffusion processes would play an important role.

Finally, the model proposed by D'Orleans and collaborators was originally used to explain the deformation of Co NP by 200-MeV iodine ions.[19] Despite the large difference in irradiation energy, we have found this model useful to understand our results, as our NPs are smaller than theirs, too. Furthermore, the size increment without deformation of Ag colloids thermally grown on SiO_2, reported by Penninkhof *et al.*,[15] can also be understood in terms of the D'Orleans and collaborators model, since the corresponding temperature in this case is in region I, as their initial NP size is smaller and the Si ions energy is higher. However, to understand the formation of NP chains, as the case where soda-lime glass was used with a higher NP concentration and a larger size distribution,[13,14] the second stage ($t > 10^{-9}$ s) is needed, since the solubility and high mobility of molten silver play an important role. Although these results support insight into the validity of the model proposed by D'Orleans and collaborators,[19] as well as in its limitations, further work is needed to draw final conclusions about the deformation mechanisms of embedded metal NPs.

V. CONCLUSIONS

In conclusion, we have verified by optical techniques that symmetric silver nanoparticles embedded in a glass matrix suffer an anisotropic deformation upon Si-ion irradiation. The optical response has been simulated, finding that nanoparticles acquired an aligned prolate spheroidal shape after irradiation, which explains the observed optical anisotropy along the direction of the Si-ion beam. As the irradiation fluence increases, the deformation also does, indicating a control of the deformation by varying the Si-ion fluence. We showed that performing a systematic experimental study of the optical response with a proper theoretical interpretation, allowed us to unambiguously determine the deformation of the particles, even when this can be so small that is difficult to observe using HRTEM. Our results bring out interesting conclusions about the NPs deformation mechanism, since the deformation of silver NPs using ion-beam irradiation is reported. The differences found between our work and previous attempts to deform silver NPs are explained in terms of a different deformation mechanism, which supports that the NP is probably melted by the ion impacts and then it flows into the ion tracks. Other recent results, where the silver NPs were not deformed, but they grew up or formed chains, can be also understood within this model in terms of the temperature reached by the nanoparticle because of its size. It is expected that this information would be useful to motivate further theoretical and experimental studies to unambiguously understand the deformation mechanism of embedded metal nanoparticles.

ACKNOWLEDGMENTS

We acknowledge the fruitful discussions with Ignacio L. Garzón. Partial financial support from CONACyT Grants No. 48521-F, No. 40122, No. 42823-F, and No. 42626-F, and DGAPA-UNAM Grants No. IN101605 and No. IN-104303 is acknowledged. K. López, F. J. Jaimes, J. G. Morales, L. Rendón, and J. Arenas are also acknowledged. HRTEM images were obtained in the Central Microscopy Laboratory of the Instituto de Física at UNAM.

*Electronic address: cecilia@fisica.unam.mx

[1] W. L. Barnes, A. Dereux, and T. W. Ebbesen, Nature (London) **424**, 824 (2003).

[2] S. A. Maier, P. G. Kik, H. A. Atwater, S. Meltzer, E. Harel, B. E. Koel, and A. A. G. Requicha, Nat. Mater. **2**, 229 (2003).

[3] K. L. Kelly, E. Coronado, L. L. Zhao, and G. C. Schatz, J. Phys. Chem. B **107**, 668 (2003).

[4] C. Noguez, Opt. Mater. (Amsterdam, Neth.) **27**, 1204 (2005).

[5] F. Gonella and P. Mazzoldi, *Handbook of Nanostructured Materials and Nanotechnology*, edited by H. S. Nalwa (Academic, New York, 2000), Vol. 4, Chap. 2, p. 81.

[6] J. Roiz, A. Oliver, E. Muñoz, L. Rodríguez-Fernández, J. M. Hernández, and J. C. Cheang-Wong, J. Appl. Phys. **95**, 1783 (2004).

[7] R. F. Haglund, L. Yang, R. H. Magruder III, J. E. Wittig, K. Becker, and R. A. Zuhr, Opt. Lett. **18**, 373 (1993).
[8] P. Figliozzi, L. Sun, Y. Jiang, N. Matlis, B. Mattern, M. C. Downer, S. P. Withrow, C. W. White, W. L. Mochán, and B. S. Mendoza, Phys. Rev. Lett. **94**, 047401 (2005).
[9] M. L. Brongersma, E. Snoeks, T. van Dillen, and A. Polman, J. Appl. Phys. **88**, 59 (2000).
[10] T. van Dillen, E. Snoeks, W. Fukarek, C. M. van Kats, K. P. Velikov, A. van Blaaderen, and A. Polman, Nucl. Instrum. Methods Phys. Res. B **175-177**, 350 (2001).
[11] T. van Dillen, A. Polman, C. M. van Kats, and A. van Blaaderen, Appl. Phys. Lett. **83**, 4315 (2003).
[12] S. Roorda, T. van Dillen, A. Polman, C. Graf, A. van Blaaderen, and B. J. Kooi, Adv. Mater. (Weinheim, Ger.) **16**, 235 (2004).
[13] J. J. Penninkhof, A. Polman, L. A. Sweatlock, S. A. Maier, H. A. Atwater, A. M. Vredenberg, and B. J. Kooi, Appl. Phys. Lett. **83**, 4137 (2003).
[14] L. A. Sweatlock, S. A. Maier, H. A. Atwater, J. J. Penninkhof, and A. Polman, Phys. Rev. B **71**, 235408 (2005).
[15] J. J. Penninkhof, T. van Dillen, S. Roorda, C. Graf, A. van Blaaderen, A. M. Vredenberg, and A. Polman, Nucl. Instrum. Methods Phys. Res. B **242**, 523 (2006).
[16] J. C. Cheang-Wong, U. Morales, A. Oliver, L. Rodríguez-Fernández, and J. Rickards, Nucl. Instrum. Methods Phys. Res. B **242**, 452 (2006).
[17] P. B. Johnson and R. W. Christy, Phys. Rev. B **6**, 4370 (1972).
[18] C. Noguez, J. Phys. Chem. B (unpublished).
[19] C. D'Orléans, J. P. Stoquert, C. Estournès, C. Cerruti, J. J. Grob, J. L. Guille, F. Haas, D. Muller, and M. Richard-Plouet, Phys. Rev. B **67**, 220101(R) (2003).
[20] J.-M. Lamarre, Z. Yu, C. Harkati, S. Roorda, and L. Martinu, Thin Solid Films **479**, 232 (2005).
[21] S. Klaumünzer, Nucl. Instrum. Methods Phys. Res. B **244**, 1 (2006).
[22] H. Trinkaus and A. I. Ryazanov, Phys. Rev. Lett. **74**, 5072 (1995).
[23] T. van Dillen, A. Polman, P. R. Onck, and E. van der Giessen, Phys. Rev. B **71**, 24103 (2005).
[24] J. C. Cheang-Wong, A. Oliver, J. Roiz, L. Rodríguez-Fernández, J. M. Hernández, and A. Crespo-Sosa, J. Phys.: Condens. Matter **13**, 10207 (2001).